Research Journal of Applied Sciences, Engineering and Technology 8(16): 1781-1786, 2014
DOI:10.19026/rjaset.8.1165
ISSN: 2040-7459; e-ISSN: 2040-7467

Submitted: March 13, 2014 Accepted: April 26, 2014 Published: October 25, 2014

Research Article

Gravity Propelled Low Temperature Engine

Ikechi Ofong, Nnamdi V. Ogueke, Emmanuel E. Anyanwu and David C. Onyejekwe
Department of Mechanical Engineering, Federal University of Technology, PMB 1526, Owerri, Nigeria

Abstract: The aim of this study is to improve the performance of a gravity propelled low temperature engine. It consists of four concentric cylindrical tanks pairs, operating with two fluids, water and 1, 1, 1, 2-tetrafluoroethane (R-134a). The inner tank holds water which is responsible for producing rotation while the annulus between the concentric cylindrical tanks holds R-134a which vaporizes and produces the vapour pressure that moves water from lower to upper tank mates. Wheel rotation is achieved when the water mass falls by gravity from this height. The inner tanks of the tank pairs are linked by a pipe through which the working fluid is transferred. The entire assembly forms a power wheel of 1.5 m diameter. Heat energy is provided by warm water at 50°C contained in a trough located at the bottom of the wheel. Test results reveal that an average wheel speed of 2.5-3.0 rpm is possible, representing a performance improvement of over 500%. This corresponds to a possible power generation of 30-35 W. Thus power generation from this engine is possible and has the potential to serve as a good alternative power source in remote locations without grid connected electricity.

Keywords: Engine, gravity propelled, low temperature, power

INTRODUCTION

Conventional heat engines are powered by the high temperature combustion of hydrocarbon fuels. The operation is usually associated with environmental damage resulting from the combustion process and the release of harmful pollutants that threaten the existence of life itself. Again, the trend of the increasing cost of these fuels is a measure of their scarcity. This can be attributed to the soaring exploration and production costs in the wake of the rapid depletion of these energy sources. Against this backdrop, any heat engine whose operation can overcome the above challenges is certainly a welcome development. This will ensure a damage-free environment, while conserving finite energy resources. A possible approach to solving this problem is the development of engines powered entirely by renewable energy.

Some progress has been reported in this direction. This is power generation from steam turbine powered by solar energy. Successful power generation using this process have been reported (Kribus *et al*., 1998; Mills and Morrison, 1999). Some power plants using this principle have been installed in Spain, United States, Australia and Crete. This however involves a complicated circuit of solar collectors, pipes and turbines and it is also expensive, thus ruling out the possibility of the full dependence on it for extension of power to rural areas or poor countries. Furthermore, it operates at very high temperature. This is possibly responsible for the increasing attention to the Stirling engine; an external combustion engine that operates at much lower temperature and has the capability of utilizing any source of heat, including solar and biomass. They are simple and safe to operate and run almost silently (Senft, 1993). Several authors have reported their work on the Stirling engine. They include those by Kolin *et al*. (2000) and Senft (2004), who first showed the possibility of power generation from low temperature difference Stirling engine; Karabulut *et al*. (2009) on low and medium temperature heat source β-type Stirling engine; Cheng and Yang (2012) who used theoretical method to optimize the geometrical parameters of Stirling engine; Kongtragool and Wongwises (2007) on the performance of low-temperature differential Stirling engine; and Kolin *et al*. (2000) who worked on electricity production from Stirling engine powered by geothermal energy source. Kongtragool and Wongwises (2003) also carried out a comprehensive review of solar powered and low temperature differential Stirling engines. These studies show that heat source temperature above 90°C is required for the engine to work. Furthermore, the power output is quite dependent on the heater temperature. Since most simple solar collectors cannot produce this high heat source temperature, the use of solar collector for this system will still require some complicated solar collector circuit and solar concentrators. Also, Stirling engines still have complicated combination of crank shaft, piston, connecting rod, etc., arrangement as obtains in a typical internal combustion engine.

Corresponding Author: Nnamdi V. Ogueke, Department of Mechanical Engineering, Federal University of Technology, PMB 1526, Owerri, Nigeria, Tel.: +234 805 300 6458

Another possibility, though not extensively tested, is that based on the principle demonstrated by Mintos in the early 1970's (Lindsle, 1976). This is a high torque low speed engine. In this engine, successive evaporation and condensation of a working fluid produced revolution which could be used to produce power, if coupled to a generator, or used directly to drive a mechanical device. Its attraction comes from the fact that a temperature of 10-15°C above ambient can effectively power it. Consequently solar energy and other low grade heat sources can be conveniently utilized to power it. When solar energy is considered, the simple flat plate collector could be used. The initial demonstration yielded RPM less than 1.00. This was attributed to poor heat transfer and the number and size of tanks employed (Hegerberg, 2001). In an analysis of a system built by Mother Earth News in USA, Tharp (2004) observed that the heat transfer rate at the source is about 40 times greater than that at the sink, thus exposing all the fluid to the heat source with the high heat transfer and trying to cool it with a lower heat transfer rate at the sink resulted in the recorded poor performance. He therefore recommended that bulk of the working fluid should be isolated or shielded from heating by using double tank or rectangular tank.

Apart from heat transfer and tubes size/ configuration considerations, the effect of working fluid was also considered (Hegerberg, 2001). This led him to recommending some common refrigerants as the most efficient for use. However, environmental concern ruled them out. Considering the narrow vapourization-condensation temperature differential, Rhodes (2001) recommended the use of Methylene Chloride (CH_2Cl_2) as the working fluid. Unfortunately CH_2Cl_2 reacts with moisture to form hydrochloric acid, hence the connecting tubes and tanks can easily be attacked by the resulting acid.

In this study, a concentric cylindrical tube arrangement with two different fluids was employed with the aim of improving the performance of the system. While one of the fluids is in direct contact with the heat source and sink and consequently vaporizes and condenses, the other fluid operates without getting heated and thus remain unchanged throughout.

MATERIALS AND METHODS

Figure 1a and b show the picture and isometric drawing of the engine, respectively. It consists of four cylindrical tank pairs arranged as shown in the figures, with each pair consisting of an outer tank 100 mm OD, 98 mm ID and an inner one 95 mm OD, 75 mm ID which is concentric to the outer tank. Both are 600 mm long. The two oppositely placed tanks are linked by 55 mm OD, 50 mm ID PVC pipes. The outer tank is made from steel, for enhanced heat transfer from the warm water which acts as the heat source to the fluid inside the tank, while the inner tank is made from PVC

Fig. 1a: Photographic view of the engine

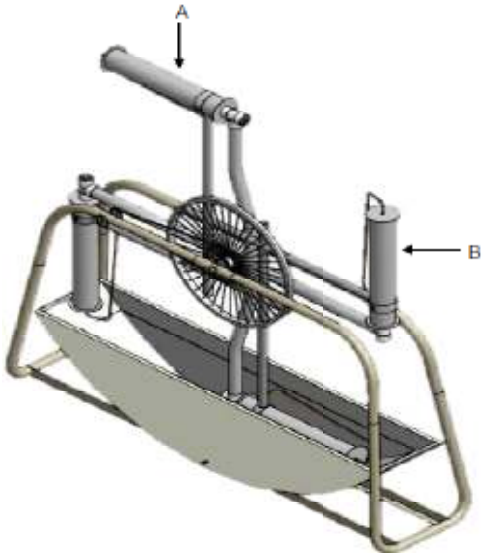

Fig. 1b: Isometric drawing of the engine

material to minimize direct heating of its content. The annulus space between the inner and outer tank contains one of the working fluids ((1, 1, 1, 2-tetrafluoroethane (CH_2FCF_3) -R134a), which undergoes phase change thus providing the needed pressure to shift the other fluid (Water (H_2O)) held in the inner tank that provides the weight required for the engine to spin. Heat to drive the system is obtained from warm water at 50°C contained in a trough of cylindrical section with a radius of curvature 1200 mm. The open surface dimensions are 1800×320 mm. This configuration ensures that the tanks will ride in and out of the trough without any obstruction.

Each tank pair is welded across a bicycle wheel of diameter 650 mm (complete with hub and spokes) using steel pipes 36 mm OD. Adjacent tank pairs are placed 90° to each other, to yield a centreline diameter of 1500 mm. The entire tank assembly now on a wheel, is mounted via the hub on a tubular steel structure, with the water trough mounted on its base. A digital tachometer is used to measure the speed of rotation of the engine while the eventual output speed is increased through a chain-sprocket arrangement to a desired speed. Detailed description of the processes involved in this use of two fluids is a subject of a patent being processed. Technical specifications of the prototype engine are presented in Table 1.

Table 1: Technical details of the engine

Component	Material specification	Dimension (mm) d_0	d_i	L	Volume (m^3)
R134a tank	Steel	100	98	600	0.0003 (annulus)
Water tank	PVC	95	75	600	0.0025
Transfer pipe	PVC	55	50	1500	0.0025
Water trough	Steel	L×W×H 1800×320×400 mm			
R134a tank heat transfer area (m^2):		0.789			
Overall heat transfer coefficient (W/m^2 K)		1355 (heat source)			601 (heat sink)
Heat transfer rate (kW)		21.380 (heat source)			9.48 (heat sink)
Heat source temperature (^oC)		50			
Wheel diameter (mm)		1500			
Mass of water (kg)		5			
Mass of R134a (kg)		0.250			

d_o: Outer diameter; d_i: Inner diameter; L: Length

The entire system was tested for leaks by pressurizing to 2.7 bar. If after 24 h the pressure remained above or equal to 2.65 bar, the system was considered perfectly sealed. Upon confirmation of leak proof, the entire system was evacuated with a vacuum pump in order to remove non condensable gases, like air. This was followed by the introduction of 0.0025 m^3 of water into two of the inner tanks (i.e., tanks "A" and "B" in Fig. 1b). Thereafter, each of their annulus space was charged with 140 g of R-134a. The water trough was then filled with warm water at 50°C. Gauge manifold with compound (low pressure and vacuum) and high pressure gauges was used for the leak testing, evacuation and charging.

On completion of leak testing, evacuation and charging, one of the tanks "A" was shifted gently until it was submerged in the warm water trough. The entire system was restrained from turning, during which time all the water in the inner tank for that submerged was shifted to the opposite tank. The system was allowed to start turning on its own, while the rpm was measured every 5 min using a tachometer. Also engine power developed corresponding to the measured rpm was evaluated using Eq. (1):

$$P = W_c \frac{(rpm)}{60} \quad (1)$$

and,

$$W_c = \rho v_{H_2O} ngD \quad (2)$$

where,

ρ (kg/m^3) and v (m^3) = The density and volume of water, respectively
n = The number of tank pairs
g (m/s^2) = The acceleration due to gravity
D (m) = The wheel diameter
W_c = The cyclic work (J)

RESULTS AND DISCUSSION

Results obtained from the system for five different engine speed test runs are presented in Fig. 2. It can be seen from the figures that all results present similar performance trend. At the start, the rpm was high with values in the range of 5.0-6.5. This value gradually dropped until it stabilized between 2.5-3.0 rpm.

This observed trend may be attributed to the transition from transient to steady state mode of the wheel rotation. Initially, motion was restrained which allowed all the water mass to be transferred to the upper tank. This was to initiate rotation. Subsequently when rotation commenced, because of the speed developed, each tank spends shorter time in the warm water bath with a resultant reduction in the mass of water transferred. At the same time in the heat sink region, because of the speed and lower heat transfer rate, only a fraction of all the R-134a vaporized was condensed, thus bringing about a reduction in the R-134a available for the water transfer. The net effect is a reduction in the water transferred and a consequent reduction in rpm. This is so because the percentage of water not transferred will aim to counter the rotation caused by the percentage transferred. This is best understood from Fig. 3a and b.

Figure 3a, depicts a situation where all the water is transferred to the upper tank from the lower tank. The weight $m'g$, which acts to counter the rotation, is the weight of the empty vessels. On the other hand, Fig. 3b shows when only part of the water is transferred to the upper tank. Some is still left in the lower tank with the result that $m'g$ here represents weight of the vessels and the unmoved water. Thus it will have more effect at reducing the speed of rotation. In fact, periodic checks when the speed appears to have stabilized revealed that only about 65% of the water was transferred. In order to undertake such checks, rotation was abruptly stopped after about 15-20 min after start-up. Thus such tests were not included as part of the performance test since the aim was basically to have an idea of the proportion of water transferred. In all, three such checks were carried out.

Considering Fig. 2, point "A" explains what happens when all the water is transferred completely while region "AB" explains how the percentage not transferred affect the rotation of the engine. Thus it can be inferred that this region, which represents a speed reduction period, is the period when the vaporized R-

134a is undergoing balancing with the condensed R-134a. On the other hand region "BC", where the speed appears balanced, represents when heat transfer equilibrium has been achieved at the heat source and heat sink respectively, with the result that mass of R-134a vaporized is equal to mass condensed.

It is interesting to note that the engine begins to show evidence of balanced performance after about 10 to 15 min of start-up. This is evident from all the test results obtained. This delay may be as a result of the initial large quantity of water transferred at start-up and the consequent high angular momentum it sets up.

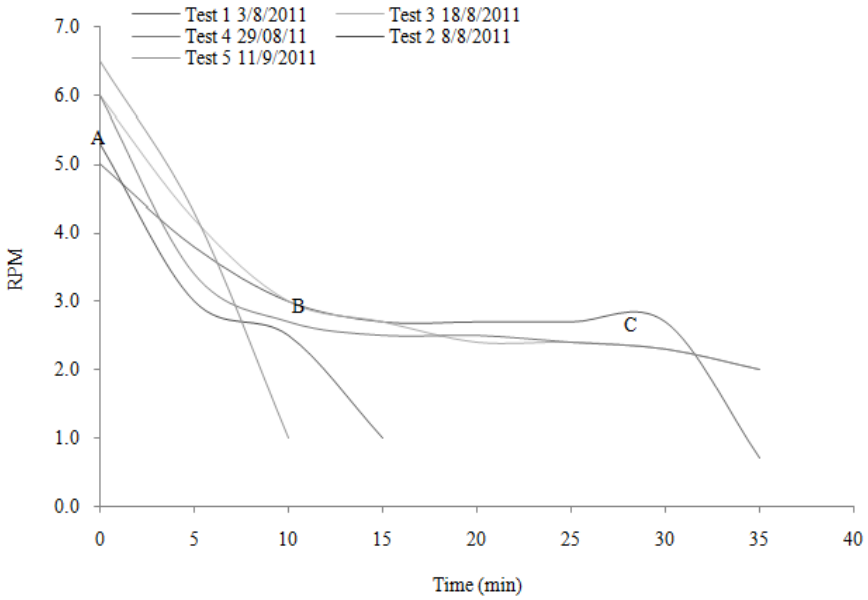

Fig. 2: Results of engine speed for five different days

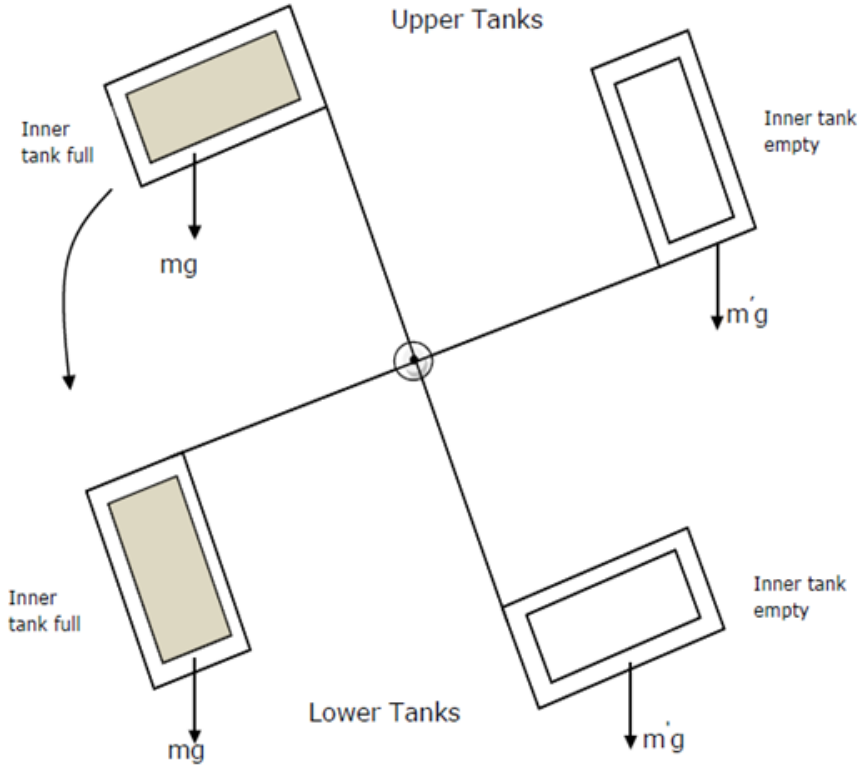

Fig. 3a: An illustration of how the engine revolution if affected by water transferred (for a case where all the water is transferred)

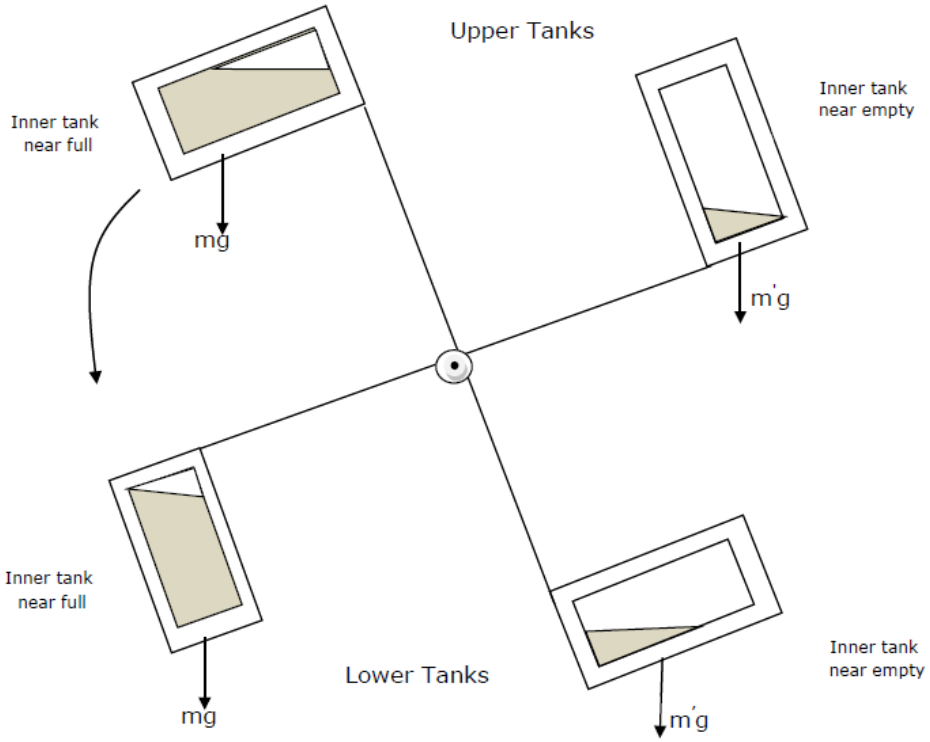

Fig. 3b: An illustration of how the engine revolution if affected by water transferred (for a case where a percentage of all the water is transferred)

Table 2: Comparison of some of the engine's performance parameters with the stirling engine

	RPM	Thermal efficiency (%)	Power (W)	Heat source temperature (°C)	Heat sink temperature (°C)
Present engine	15	0.08	35	50	30
β-type stirling engine (Kongtragool and Wongwises, 2003)	453	15	51.93	200	27
γ-type stirling engine (Kribus *et al*., 1998)	133	0.48	11.80	316	34

The engine was expected to operate for hours. However, results obtained show that engine operation was sustained for a maximum of about 35 min. This was as a result of sudden failure of the sealants used after about 35 min of operation resulting in loss of the R-134a. At present, more work is on-going in order to address this leak problem and some other identified construction issues. However, the 35 min operation revealed that with improved construction, power generation from such engine is possible.

Table 2 shows a comparison between the prototype engine and some other low temperature engines. It can be seen from the table that the engine has a good potential. This is seen from its RPM and the corresponding power at the RPM as compared to those of Karabulut *et al*. (2009) and Kongtragool and Wongwises (2007). However, the thermal efficiency is very low compared to the other two engines. The low thermal efficiency may be attributed to two reasons:

(i) Construction deficiencies
(ii) The low operating temperatures

Reason (i) was partly responsible for the low heat transfer rate at the heat sink which was responsible for a drop in RPM and consequently the derivable power. The high power corresponding to the low RPM may be attributed to the mass of water contained in the tank which is actually responsible for the rotation. Increasing this mass increases the force of rotation and thus the shaft power. This is one possible means of improving the shaft power of such engine.

CONCLUSION

A gravity propelled low temperature engine has been designed and tested. From results of performance tests conducted, the following conclusions may be drawn:

- Power generation using such a low temperature engine is possible.
- The engine tested has the capacity of turning at between 2.5-3.0 rpm. This value can be stepped-up using chain and sprocket arrangement. With further improvements in design and construction, much

higher rpm could be achieved. However the 2.5-3.0 rpm achieved is an improvement of more than 500% of the earlier Minto's wheel.

- For improved engine performance, efforts should be made towards improving the heat transfer rates especially, that at the heat sink region.
- Since the engine is driven by a low boiling point working fluid, the energy source can be obtained from any low grade heat energy source, including solar energy. Hence this low temperature engine can serve as a good alternative power source for remote locations without grid connected electricity.
- For the tested engine, power generation in the range of 30-35 W is possible when the measured wheel speed is stepped-up five times. When this is compared with the original Minto's wheel, this represents a very significant improvement with room for much further improvements.

REFERENCES

Cheng, C. and H. Yang, 2012. Optimization of geometrical parameters for Stirling engines based on theoretical analysis. Appl. Energ., 92: 395-405.

Hegerberg, B., 2001. Details for the Minto Wonder Wheel. Retrieved form: www.keelynet.com/minto/minto2.htm (Accessed on: April 22, 2014).

Karabulut, H., H.S. Yűcesu, C. Cinar and F. Aksoy, 2009. An experimental study on the development of a β-type Stirling engine for low and moderate temperature heat sources. Appl. Energ., 86: 68-73.

Kolin, I., S. Koscak-Kolin and S. Golub, 2000. Geothermal electricity production by means of the low temperature difference Stirling engine. Proceedings of World Geothermal Congress. Kyushu-Tohoku, Japan.

Kongtragool, B. and S. Wongwises, 2003. A review of solar-powered Stirling engines and low temperature differential Stirling engines. Renew. Sust. Energ. Rev., 7: 131-154.

Kongtragool, B. and S. Wongwises, 2007. Performance of low-temperature differential Stirling engines. Renew. Energ., 32: 547-566.

Kribus, A., R. Zaibel, D. Carey, A. Segal and J. Karni, 1998. A solar-driven combined cycle power plant. Sol. Energy, 62: 121-129.

Lindsle, E.F., 1976. Minto's Wonder Wheel. Popular Science. Retrieved form: http://amasci.com/freenry/minto.html (Accessed on: April 23, 2014).

Mills, D.R. and G.L. Morrison, 1999. Compact linear Fresnel reflector solar thermal power plants. Sol. Energy, 68: 263-283.

Rhodes, W.H., 2001. Use of Methylene Chloride for Minto Wheel. Retrieved form: www.keelynet.com/minto/minto2.htm (Accessed on: April 22, 2014).

Senft, J.R., 1993. Ringbom Stirling Engines. Oxford University Press, New York.

Senft, J.R., 2004. An Introduction to Low Temperature Differential Stirling Engines. Pennsylvania State University, Moriya Press, USA.

Tharp, T., 2004. Minto Wheel Calculations. Retrieved form: http:// www.borderschess.org/mintowheelcalculationupdate.pdf (Accessed on: April 23, 2014).